Materials Research Proceedings 41 (2024) 2245-2251 https://doi.org/10.21741/9781644903131-247

Methodology for the automated spatial mapping of heterogeneous elastoplastic properties of welded joints

HAMILL Robert[1,a*], MAREK Aleksander[1], HARTE Allan[2] and PIERRON Fabrice[1,3,b]

[1]Faculty of Engineering and Physical Sciences, University of Southampton, UK

[2]UKAEA, Culham Science Centre, Oxfordshire, UK

[3]MatchID NV, Ghent, Belgium

[a]r.hamill@soton.ac.uk, [b]fabrice.pierron@matchid.eu

Keywords: Welding, Virtual Fields Method, Identification, Full-Field Measurements, Heterogeneity, Materials Testing 2.0

Abstract. A methodology to map the heterogeneous elastoplastic mechanical properties of welded joints is presented. The approach and results of the proposed methodology are demonstrated using numerical data representing an off-axis butt-weld. This work extends the Virtual Fields Method (VFM) by introducing automated spatial parameterisation of the constitutive parameters. This extension enables the novel characterisation of welds with more complex geometries, loading conditions and dissimilar materials.

Introduction

Inverse identification methods have been previously developed to take advantage of the rich data provided through full-field measurements. The VFM is one such method which uses full-field strain measurements to determine constitutive parameters, and benefits from computational efficiency compared to other methods as no resolution of the direct problem is required [1,2]. The VFM has previously been used to determine the constitutive parameters of welded joints with simple butt-joint geometry, however existing work requires *a priori* spatial parameterisation of constitutive parameters [3,4]. Automated spatial parameterisation removes the necessity of *a priori* knowledge, hence enabling more complex tests to be performed.

Theory and key concepts

The Virtual Fields Method. Based on the principle of virtual work (PVW), the virtual fields method (VFM) seeks to identify constitutive parameters that satisfy the weak form of the stress equilibrium equation for a given strain field. Stress fields can be reconstructed from measured strain fields using a postulated constitutive model and an initial guess of the constitutive parameters for each. The static admissibility of these stress fields can then be checked using the PVW. The constitutive parameter map is iterated until global equilibrium is satisfied, at which point the parameter map is said to be identified.

Eq. 1 shows the simplified equation for the PVW assuming quasi-static loading of a specimen with negligible body forces. This equation expresses the local stress equilibrium equation in the weak form with the force boundary conditions accounted for. It states that the internal virtual work (IVW) and the external virtual work (EVW) must balance. σ_{ij} is the internal stress within the volume, V. T_i is the traction vector acting on the boundary surface, S.

$$\underbrace{-\int_V \sigma_{ij}\epsilon_{ij}^* \, dV}_{\text{IVW}} + \underbrace{\int_{S_f} T_i u_i^* \, dS}_{\text{EVW}} = 0 \tag{1}$$

The term u_i^* is a test function, known as the virtual displacement. This term does not require physical interpretation and merely acts as a spatial weighting function over the body. The spatial derivatives of the virtual displacement are known as the virtual strains, ϵ_{ij}^*. The virtual strains are unrelated to the physical strains and again only act as spatial weighting functions.

Ensuring constant virtual displacements at the boundaries of any unknown traction distributions allows the term u_i^* to be factored outside the integral. The tractions in the EVW term can then be simplified to only require the resultant force – a value provided by the load cell of the test machine.

In this work, the stress is assumed constant throughout the thickness and the strain data provided using digital image correlation (DIC) will take the form of discrete data points. The full-field data should have sufficient spatial resolution to approximate the surface integral as a discrete sum using the mid-point rule. Hence, the PVW can be further simplified to produce Eq. 2, where F_i is the applied force vector measured by the load cell and s^p is the surface area associated with each strain data point. From this equation, a cost function can be formed as the squared difference between external and internal virtual work, and minimized for the sought parameters.

$$-\sum_{p=1}^{nPts}\left(\sigma_{ij}^{p}\epsilon_{ij}^{*p}s^{p}\right)+u_i^*F_i=0 \tag{2}$$

Sensitivity based virtual fields (SBVFs, [5]). They are automatically generated virtual fields which adapt their spatial weighting according to each parameter's stress sensitivity in order to enhance parameter identifiability.

The equilibrium gap indicator (EGI, [6,7]). A particular formulation of virtual fields can be used to identify local discrepancies or 'equilibrium gaps' in the stress fields. Assuming kinematically admissible strain fields and correctly defined thicknesses, these equilibrium gaps (local regions of inadmissible stress states) arise due to incorrect constitutive model or parameters. As such, the EGI can be used as a metric to assess spatial regions in which equilibrium is not satisfied. Previously, this formulation has been used to detect damage and to assess heterogeneity in specimens of smoothly varying stiffness. In this work the EGI is used both to identify the location of discrepancies in the parameter map and their relative magnitude. To do this, an inspection window is rastered across the stress field with virtual fields defined to negate any external work contribution from outside of the window boundary. The EGI only assesses stress equilibrium within each window, hence it evaluates if the spatial distribution of stress satisfies static admissibility. However, it is ignorant of the magnitude of applied force and hence stress levels (*i.e.* all datapoints in the stress field may be wrong by some factor but the EGI will not detect any issue providing the distribution is correct).

The force reconstruction error (FRE). Like the EGI, the FRE is another virtual field formulation which checks for the equilibrium of any cross-section with the applied load.

Eq. 3 shows how the reconstructed force for a given slice, F_r^{slice}, can be computed from the average longitudinal stresses of that slice, σ_{ii}, and its cross-sectional area, A^{slice}. Here, index i denotes the longitudinal direction of the specimen, in which the resultant load F_a is measured. The FRE value is expressed as in Eq. 4.

$$F_r^{slice}=\int_A\sigma_{ii}^{p}dA\ =h\int_L\sigma_{ii}^{p}dL\ =A^{slice}*\overline{\sigma_{ii}} \tag{3}$$

$$FRE=F_a-\ F_r^{slice} \tag{4}$$

Spatial parameterisation. In order to reconstruct the stress fields from the measured strain fields, we need to assign a value for each constitutive parameter at every point in our dataset. However, this spatial map of parameters is unknown and to be identified, so a parameterisation scheme is

required to reduce the number of unknowns to an acceptable level. The parameterisation scheme will reconstruct a spatial map of values for each constitutive parameter from a number of variables (less than the number of datapoints). To date, this problem has been tackled by manually discretising the specimen into subregions *a priori* and then assuming each subregion is homogeneous (*e.g.* [3,4]). However, *a priori* information about the spatial distribution of properties is not always known, and automating spatial parameterisation would enable novel characterisation of specimens with more complex geometries and loading conditions.

A mesh is perhaps the most intuitive parameterisation approach. Each datapoint is assigned a value depending on its position within the element it lies in. Degrees of freedom define the nodal values and shape functions are used to specify the distribution of values throughout the element. The mesh can be refined by changing the number of elements or by changing the order of the shape functions. However, meshed methods inherently required a rigid structure and the number of unknowns increases rapidly with refinement.

Meshless approaches can provide greater flexibility, and radial basis functions (RBFs) are used in this work due to their flexibility and relatively low degree of freedom count. A radial function is a univariate function which returns a value dependent only on the distance from the kernel origin to the point being evaluated. Multiple basis functions are combined, using the principle of superposition, to approximate the desired interpolated solution. This is the method used here.

Method

The key concepts outlined above can be combined in such a way to extend the VFM to include the automated spatial parameterisation of the constitutive parameters. This process is outlined in Fig. 1. The dashed box encloses the core VFM which, as previously described, identifies a map of constitutive parameters that best satisfies global equilibrium for a particular spatial parameterisation scheme. The EGI and FRE metrics can then be used to assess and update the parameterisation scheme. The particulars of how this is done could be modified, however the pseudo-code below outlines the approach used in this work. The core methodology will be presented through a worked example, in which synthetic data is used to mimic that obtained experimentally.

ALGORITHM 1: PSEUDO-CODE FOR HETEROGENEOUS IDENTIFICATION METHODOLOGY

```
prepare test data
prepare homogeneous baseline data
perform initial identification with mesh parameterisation and SBVF
initialise RBF parameterisation using initial identified results
perform identification with RBF parameterisation and local equilibrium metric VFs
while optimisation not converged do
    update RBF parameterisation and proceed with identification
end while
```

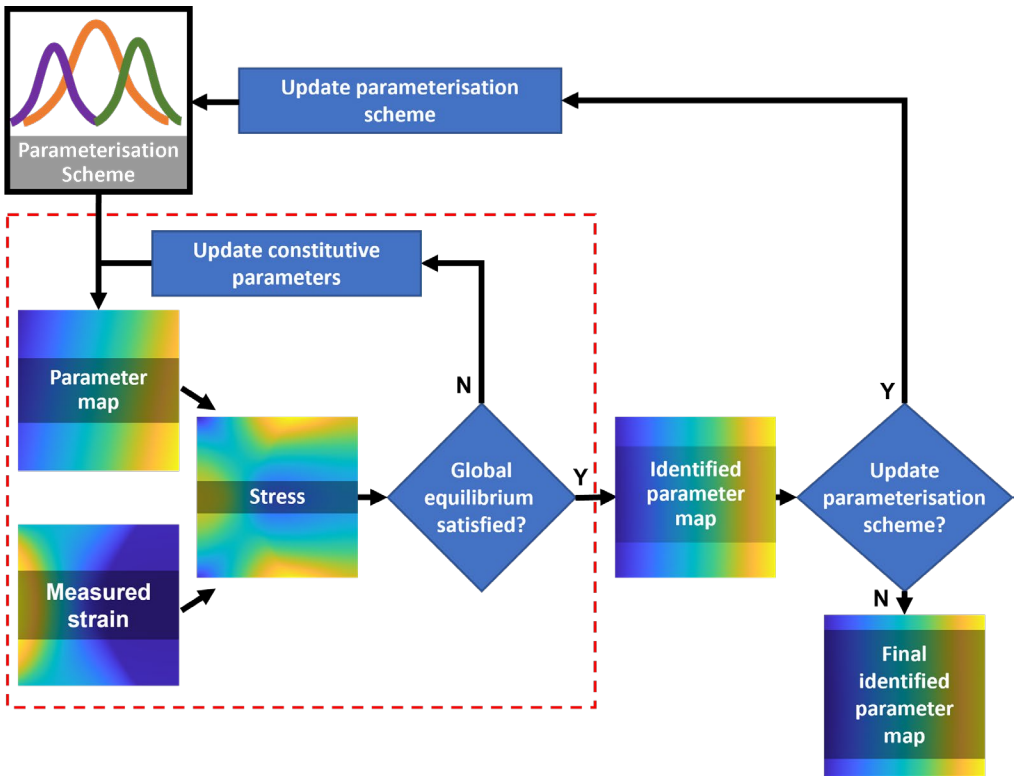

Figure 1 – The virtual fields method with automated spatial parameterisation.

Worked example

Test data generation. A notched, off-axis, butt-weld geometry is selected for the worked example (see Fig. 2). The weld region and heat affected zones have a width of 5.2 mm and 1.7 mm respectively. The off-axis angle is 60 degrees from the specimen longitudinal axis, and two offset notches penetrate the specimen 2 mm on either side. A linear hardening model is used together with Von Mises yield surface. Throughout the identification the elastic properties are assumed known, with a Young's modulus of 190 GPa and Poisson's ratio of 0.28. The yield stress will be identified as a heterogeneous parameter, and has a value of 360 MPa in the base metal and 420 MPa in the weld metal, with a linear variation throughout the heat affected zone. The hardening modulus, which will be identified as homogeneous, is assigned a value of 3700 MPa. Finite Element was used to simulate the test above, and synthetic image deformation [8] was used to realistically simulate DIC measurements. In this example, grey level noise is added directly to the images, leading to a longitudinal strain noise floor of 140 microstrain.

Initial identification. In order to get an initial indication of the heterogeneous parameter maps, a coarse, zero-order mesh is used, for which all points in an element share a single value. Hence, for the yield stress, the number of unknowns is equal to the number of elements. Initial mesh size is a user-choice, and here is set to be two elements in the vertical direction and six elements in the horizontal direction, giving a total of twelve unknowns governing the yield stress parameter map. The hardening modulus is assigned a single degree of freedom, giving thirteen unknowns in total. An initial guess of 350 MPa and 3000 MPa is assigned to the yield stress and hardening modulus respectively. The initial identification is performed using SBVFs and a gradient-descent optimizer. This results in a hardening modulus of 3296 MPa and a yield stress map as shown in the top row of Fig. 3.

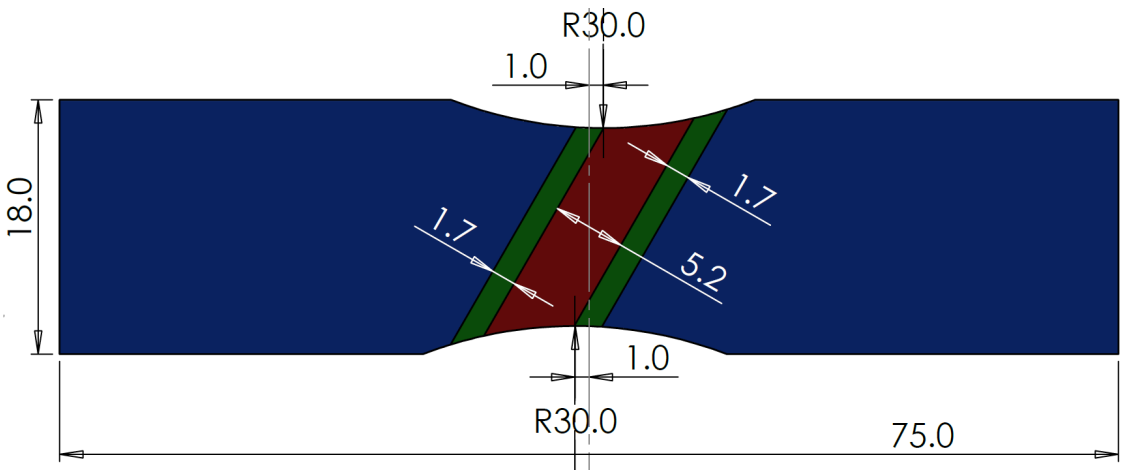

Figure 2 –Notched, off-axis butt-weld geometry. Dimensions in mm.

Initialise meshless parameterisation. The initial identification results can now be used to initialize the RBFs by fitting the RBFs to the identified parameter map (minimising the root mean squared error). The process of initially identifying using a coarse mesh and then fitting RBFs is not necessary, however, it quickly provides an approximate parameter map from which to start the global optimisation with RBFs.

Identification using RBF, EGI and FRE. Using the fitted RBF map as a starting point, identification is performed using a global optimiser to minimise a cost function composed of the normalised EGI and FRE terms. The EGI returns a 2D spatial array of values for each timestep. In this work, the root mean square of all spatial-temporal values is normalised by the baseline EGI obtained from a homogeneous case. The FRE returns a 1D spatial array, which can be extrapolated to a 2D array for each load step. Once again, the root mean square of all spatial-temporal values is normalised by the baseline FRE value. In this work, the pattern search algorithm is used, however, other optimisers such as genetic algorithms have also been used successfully.

Updating parameterisation and checking convergence. If there is no improvement after an iteration, a second attempt is made with the same number of kernels but a different starting point. If a second attempt has already been tried, the identification is ended. If there is an improvement in the cost function and the EGI and FRE metrics are below the baseline threshold, then the identification is ended, as no further improvement is feasible. Alternatively, if there is an improvement in the cost function, and the baseline threshold has not yet been reached, the parameterisation scheme is updated. To update the parameterisation, a new kernel is added to any heterogeneous parameters. This new kernel is positioned using the EGI and FRE, which highlight regions with the largest inconsistences in the stress field.

Results and discussion

The results are reported in Fig. 3 below. They clearly show how the process is able to automatically converge towards the solution without any *a priori* information on the distribution of the properties. This is a great strength of the technique compared to previously published work where such a complex distribution would not have been possible to identify without any *a priori* parameterisation, as in [3]. The method seems robust to realistic camera noise, and computational times are reasonable, about 4 hours on an Intel® Core™ i7-9700 CPU at 3 GHz with 32 Gb of RAM, with an unoptimized and unparallelised Matlab code.

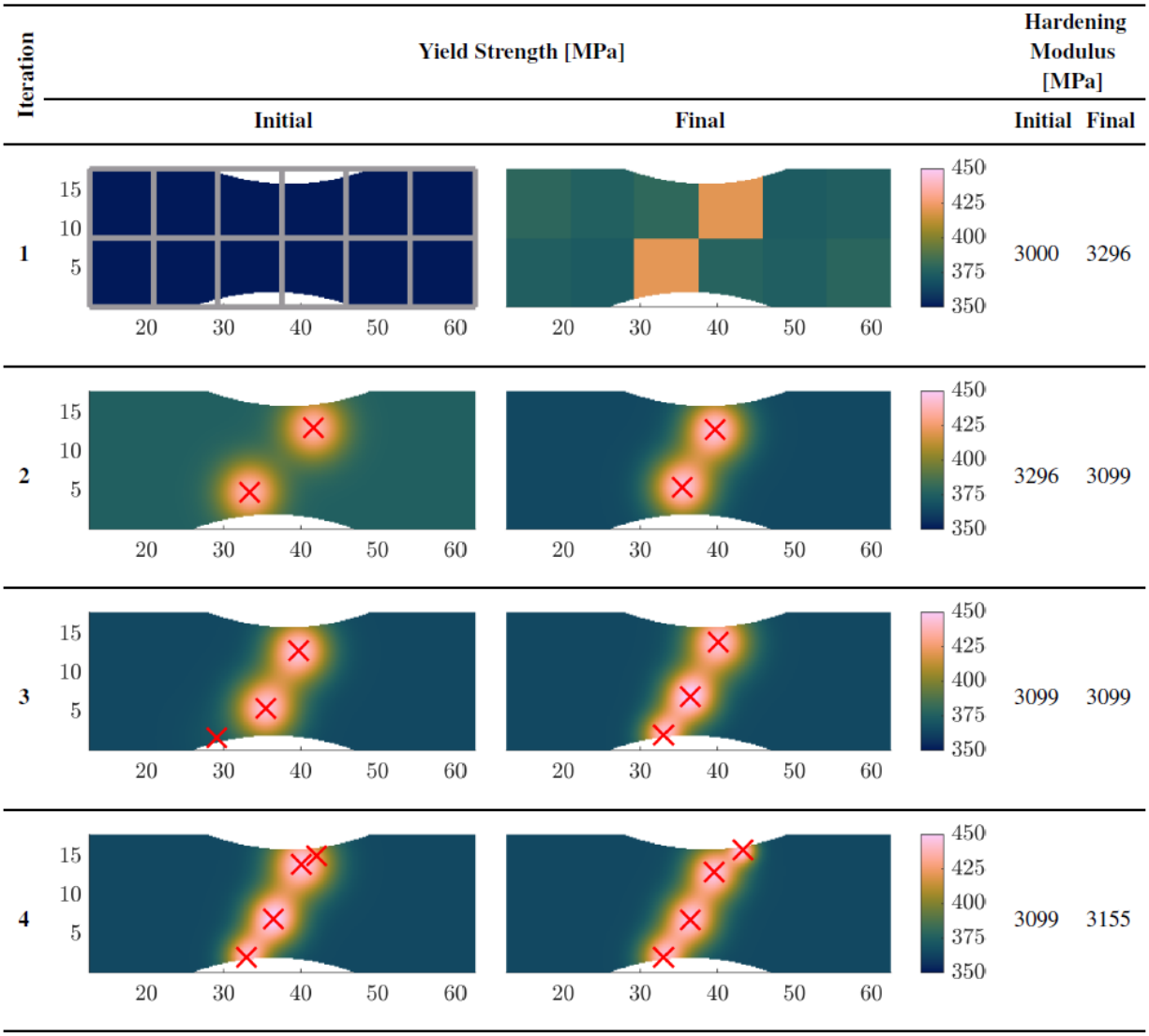

Figure 3 - Results.

Conclusion and future work

The present results are first steps towards an operational tool. Improvements can include the use of bivariate RBFs (with different 'lengths' in two orthogonal directions) instead of univariate ones. There is a question about the possibility to also identify a hardening modulus map but considering the low sensitivity of hardening, this is an open question. Finally, experimental validation is currently being performed on a butt weld with notches and then, on a T-joint.

References

[1] F. Pierron and M. Grédiac, The Virtual Fields Method, Springer, 2012. https://doi.org/10.1007/978-1-4614-1824-5

[2] J. Martins, A. Andrade-Campos, and S. Thuillier, "Comparison of inverse identification strategies for constitutive mechanical models using full-field measurements," International Journal of Mechanical Sciences, 145 (2018) 330–345, 2018, https://doi.org/10.1016/j.ijmecsci.2018.07.013

[3] M. A. Sutton, J. H. Yan, S. Avril, F. Pierron, and S. M. Adeeb, "Identification of heterogeneous constitutive parameters in a welded specimen: Uniform stress and virtual fields methods for

material property estimation," Experimental Mechanics, 48 (2008) 451–464, http://dx.doi.org/10.1007/s11340-008-9132-6

[4] G. L. Louedec, F. Pierron, M. A. Sutton, and A. P. Reynolds, "Identification of the local elasto-plastic behavior of FSW welds using the virtual fields method," Experimental Mechanics, 55 (2013) 849–859.

[5] A. Marek, F.M. Davis and F. Pierron, "Sensitivity-based virtual fields for the non-linear virtual fields method", Computational Mechanics, 60 (2017) 409-431, http://dx.doi.org/10.1007/s00466-017-1411-6

[6] C. Devivier, F. Pierron, and M. Wisnom, "Impact damage detection in composite plates using deflectometry and the Virtual Fields Method," Composites Part A: Applied Science and Manufacturing, 48 (2013) 201–218, http://dx.doi.org/10.1016/j. compositesa.2013.01.011

[7] J. Considine, F. Pierron, K. Turner, P. Lava, and X. Tang, "Smoothly varying inplane stiffness heterogeneity evaluated under uniaxial tensile stress," Strain, 53 (2017) e12237, http://dx.doi.org/10.1111/str.12237

[8] M. Rossi, P. Lava, F. Pierron, D. Debruyne, M. Sasso, "Effect of DIC spatial resolution, noise and interpolation error on identification results with the VFM", Strain, vol. 51, n0. 3, pp. 206-222, 2015. http://dx.doi.org/10.1111/str.12134